JOURNAL OF MATERIALS SCIENCE 14 (1979) 407–415

Structure and strength of dilute zirconium-copper martensites

S. L. WADEKAR, V. RAMAN, P. MUKHOPADHYAY
Metallurgy Division, Bhabha Atomic Research Centre, Trombay, Bombay 400 085, India

The morphology, the substructure and the strength of dilute zirconium–copper martensites were examined. The martensites were of the dislocated lath type. The precipitation of an intermetallic phase at the lath boundaries could not be suppressed even by rapid beta-quenching. The strength of these martensites was substantially enhanced with increasing copper additions. This increased strength appeared to be due both to solid solution hardening and the distribution of precipitates at the lath boundaries. The work-hardening behaviour of these martensites could be analysed in terms of Ashby's theory of the deformation of plastically inhomogeneous materials.

1. Introduction

The strengthening associated with the martensitic transformation arises from the contribution of several factors like solid-solution hardening, precipitation hardening, order hardening and substructure hardening. The effects of these factors often overlap, making the assessment of the individual contributions quite difficult. Heat treatments involving the martensitic reaction have been found to be quite effective in strengthening zirconium and titanium alloys.

Zirconium–copper alloys, with and without ternary additions, are possible materials for use in nuclear reactor technology. Dilute binary zirconium–copper alloys and ternary alloys like Zr–(0.5 to 3 wt%) Cu–(0.5 to 3 wt%)V and Zr–0.5 wt% Cu–0.5 wt% Mo have been considered as fuel cladding materials in the temperature range of 500 to 600° C in gas-cooled reactors [1–4]. The work described in this paper was undertaken with a view to examining the influences of solution hardening and of intermetallic precipitate distribution on the strength of dilute zirconium–copper martensites. Since the equilibrium solubility of copper in alpha-zirconium is extremely limited [5], a significant extent of solute supersaturation could be achieved, even in very dilute alloys, by quenching rapidly from the beta-phase field.

2. Experimental procedure

The alloys used in this study (Zr–0.1 wt% Cu, Zr–0.2 wt% Cu, Zr–0.4 wt% Cu and Zr–0.75 wt% Cu with interstitial levels in the range 950 to 1000 ppm) were prepared by melting weighed amounts of nuclear grade sponge zirconium and high purity copper in a nonconsumable arc furnace. The fingers were initially hot rolled and subsequently cold rolled till a final thickness of about 0.3 mm was attained. Samples obtained from these strips were wrapped in tantalum foil and encapsulated in silica capsules under a protective atmosphere of helium at about 175 mm Hg pressure. These samples were beta-solutionized at 950° C for 30 minutes and subsequently water quenched rapidly. Tensile tests were carried out in an Instron tester at the desired temperatures, using a strain rate of 6.5×10^{-5} sec^{-1}. X-ray diffraction was carried out using a monochromated copper Kα radiation. For transmission electron microscopy, thin foils were obtained by a multistage procedure involving mechanical grinding, chemical thinning and electropolishing (using the "window technique"). The electropolishing solution contained 30 parts of perchloric acid, 175 parts of *n*-butanol and 300 parts of methanol. The electrolyte temperature was maintained below −50° C and voltages in the range of 20 to 30 V were used. Examination of the thin foils was carried out in a

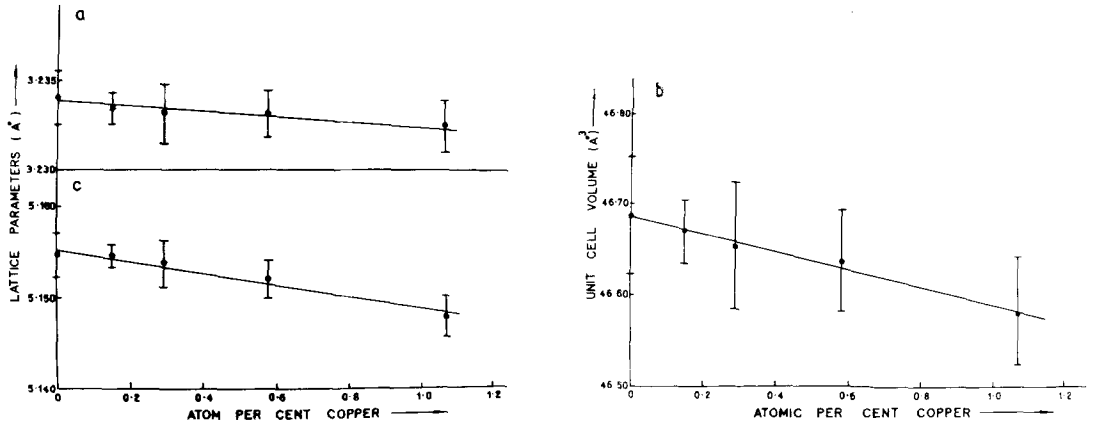

Figure 1 Plots showing the decreasing trend in (a) the lattice parameters and (b) the volume of the α-Zr (Cu) unit cell with increasing copper content in dilute zirconium–copper alloys.

Siemens Elmiskop 102 microscope, operating at 125 kV.

3. Results and discussions

3.1. Structure of the beta-quenched alloys

X-ray diffraction from all the beta-quenched alloys showed only alpha-zirconium peaks. There was a detectable decrease in the lattice parameters and, therefore, in the volume of the unit cell of the supersaturated α-Zr (Cu) solid solution with increasing copper content (Fig. 1). Transmission electron microscopy showed that beta-quenching induced the martensitic transformation in all the alloys to produce the hexagonal close packed alpha-prime phase. No evidence of a partial retention of the beta-phase could be obtained. The observed martensite morphology was of the lath type, the alpha-prime phase being constituted of blocks or packets of laths. In all the alloys the lath boundaries were found to be decorated with particles of a second phase. However, precipitates were seldom observed in the interior of the laths. These features are illustrated in Fig. 2. A conclusive identification of the precipitate phase as Zr_2Cu (the intermetallic phase richest in zirconium) was not possible by selected area diffraction. A lamellar arrangement of the lath boundary precipitates was found in some places, particularly in the Zr–0.75 wt % Cu alloy (Fig. 3). Selected area diffraction patterns obtained from neighbouring laths belonging to the same packet showed that the misorientation between these was invariably small. This implied that the lath boundaries, which appeared to consist of arrays of dislocations (Fig. 4) were small angle boundaries. The boundary dislocations were in strong contrast when imaged with the (0 0 0 2) and the $\{1\,1\,\bar{2}\,0\}$ reflections, showing that these were of the "c + a" type.

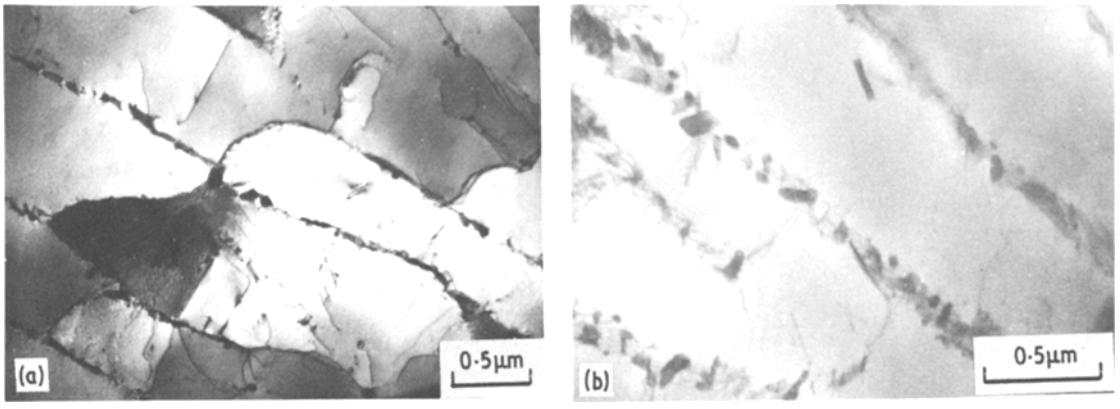

Figure 2 Typical lath martensite structure in (a) Zr–0.2 wt % Cu and (b) Zr–0.75 wt % Cu alloys obtained on beta-quenching. The presence of precipitates at the lath boundaries could be noticed.

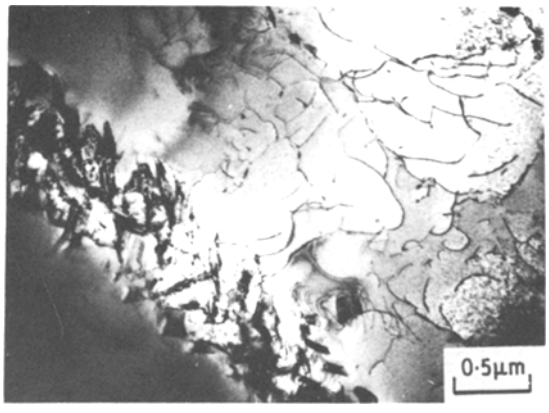

Figure 3 A lamellar arrangement of the precipitates at a lath boundary in the Zr–0.75 wt % Cu martensite.

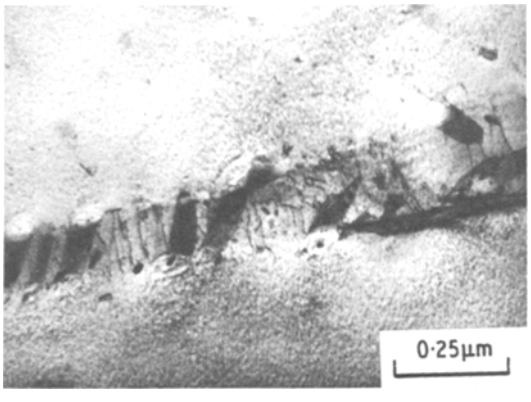

Figure 4 Lath boundary dislocations imaged in bright field with a strong (0 0 0 2) reflection operating.

The martensite laths in all the alloys has a dislocated substructure and no evidence of internal twinning of the martensite units could be obtained. The density of the intra-lath dislocations was low in most of the laths though a few crystals were found to be heavily dislocated. The fact that most of these dislocations went out of contrast when imaged with the (0 0 0 2) reflection suggested that these were of "a" type. The dislocation arrangement was, in general, irregular and only in a few cases could regular dislocation arrangements be observed. Typical dislocation structures are illustrated in Fig. 5. In the limited range of compositions studied, the average lath size appeared to decrease very slowly with increasing copper concentration. An increase in copper content was also found to result in an increase in the average size of the lath boundary precipitates as well as in their number density. At many boundaries these particles were almost contiguous, giving the impression of the formation of a thin, near continuous layer of the precipitate phase (Fig. 6).

The observed decrease in the lattice parameters of the α-Zr (Cu) solid solution with increasing copper content was expected in view of the fact that the radius of the copper atom is much smaller than that of the zirconium atom, the CN 12 radii [6] being 1.278 Å and 1.602 Å respectively (a radius misfit of over 20%). This large size difference must also be one of the major reasons why the solubility of copper in zirconium is very limited.

In view of Picklesimer's data [7] on the dependence of M_s temperature on copper concentration in dilute zirconium–copper alloys, the M_s temperature in all the alloys examined here could be taken to be above 650° C. This being the case, the observed lath morphology and absence of internal twins in the laths was consistent with the correlation proposed by Banerjee and Krishnan [8] between the M_s temperature and the morphology and substructure of zirconium alloy martensites.

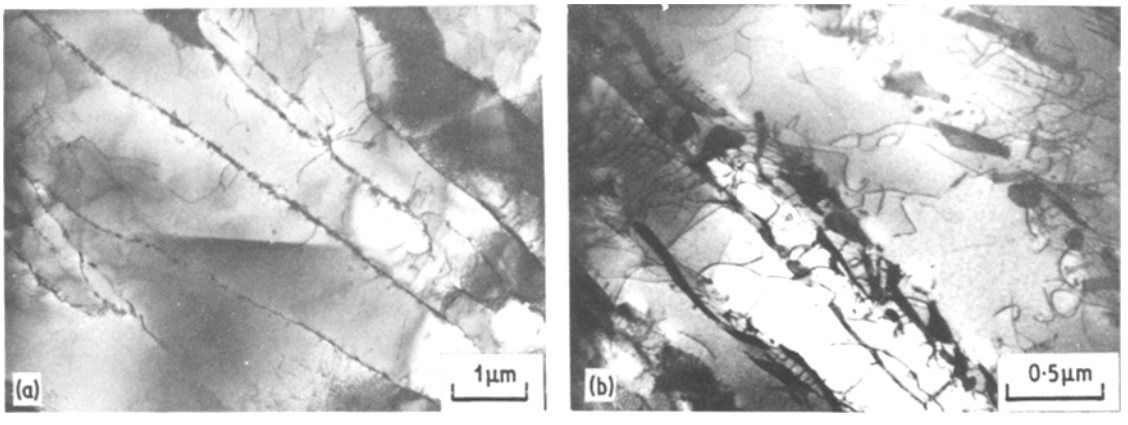

Figure 5 Typical dislocation structures within laths in (a) Zr–0.2 wt % Cu and (b) Zr–0.75 wt % Cu martensites.

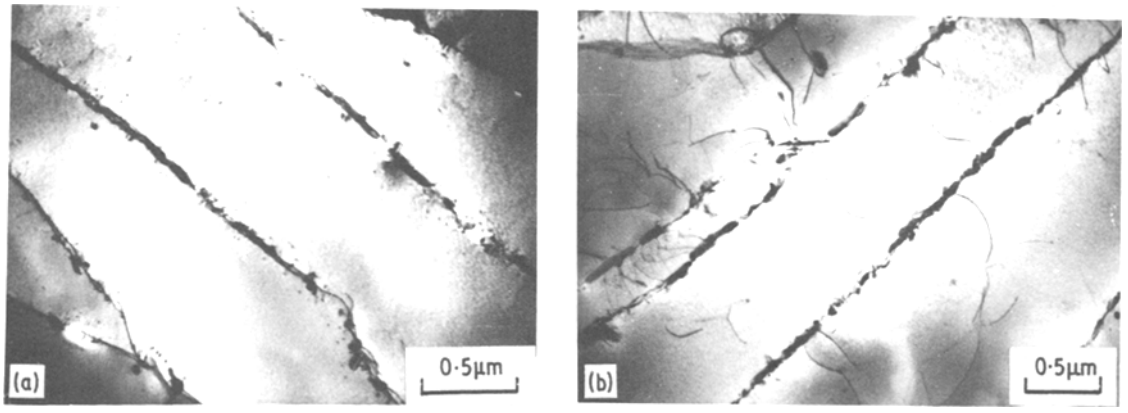

Figure 6 Thin, near continuous precipitate layers at lath boundaries in beta-quenched (a) Zr–0.2 wt % Cu and (b) Zr–0.4 wt % Cu alloys.

Again, the observations that most of the dislocations constituting the lath boundaries were of the "c + a" type while those within the laths were of the "a" type were similar to those made by Williams *et al.* [9] on dilute titanium–copper martensites.

The presence of the lath boundary precipitates indicated that the cooling rates achieved in this work were not adequate to bring about a complete martensitic transformation by fully suppressing the diffusion-controlled decomposition of the beta-phase by a nucleation and growth process. The occurrence of such precipitates has been observed in beta-quenched dilute titanium–copper alloys also and has been attributed to auto-tempering during quenching [10]. The formation of the precipitates at the lath boundaries, in preference to the lath interiors, could be due to two reasons. First, the dislocations at these small angle boundaries would enhance the nucleation of the precipitates by relieving part of the strain energy associated with their formation, thereby reducing the activation barrier for nucleation. Secondly, while the nuclei formed at the boundaries would grow by interface diffusion, those formed within the laths would have to grow with the assistance of the much slower process of volume diffusion.

Another consideration appeared to be pertinent, particularly in the context of the Zr–0.75 wt % Cu alloy where the precipitates at the lath boundaries were often found to be arranged in a lamellar fashion, suggestive of a eutectoid decomposition process. Fig. 7 depicts a simplified version of the zirconium-rich end of the zirconium–copper phase diagram, where the $\beta/\beta + \alpha$ and the $\beta/\beta + Zr_2Cu$ phase boundaries have been approximated by straight lines. If a Hultgren extrapolation is carried out by extending these two straight lines into the $\alpha + Zr_2Cu$ phase field, the region bounded by these extrapolated lines would correspond to the region of "direct eutectoid formation". In this region, under the metastable equilibrium conditions, the beta-phase would break up directly into a mixture of the alpha and the Zr_2Cu phases, without the formation of any pro-eutectoid product. A plot based on Picklesimer's data [7] on the variation of the M_s temperature with com-

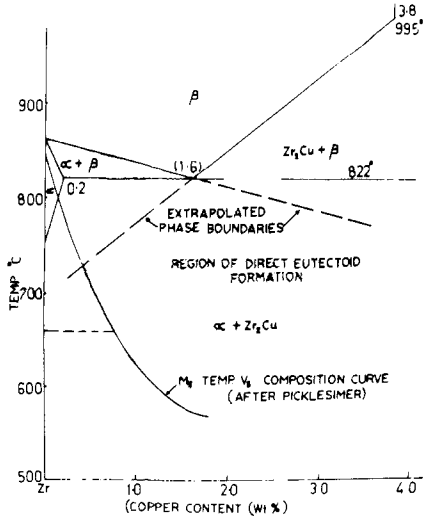

Figure 7 A simplified sketch of the zirconium-rich end of the zirconium–copper phase diagram where a linear extrapolation of the $\beta/\beta + \alpha$ and the $\beta/\beta + Zr_2Cu$ phase boundaries has been carried out in order to delineate the region of direct eutectoid formation. The variation of the M_s temperature with copper content is also shown.

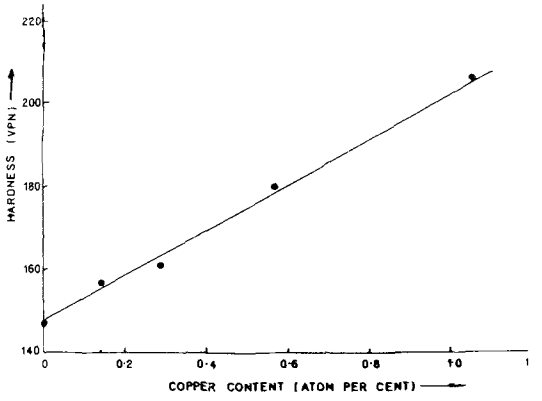

Figure 8 Plot showing the variation in hardness with copper content in dilute zirconium–copper martensites.

position in zirconium–copper alloys is superposed on the phase diagram in Fig. 7 to demonstrate that for the Zr–0.75 wt % Cu alloy, the M_s temperature lies well within the region of direct eutectoid formation. This would mean that for this composition, the supercooling necessary for initiating the martensitic reaction is also sufficient for a direct eutectoid decomposition to occur. It should be noted in this context that during beta-quenching, the alloy would "enter" the region of direct eutectoid formation at quite a high temperature where rapid diffusion would be expected to occur.

Though the quenching rates employed were insufficient to inhibit precipitation, it was inconceivable that the precipitates in the quenched alloys could have attained the Zr_2Cu stoichiometry in the course of the extremely short time available for atomic diffusion to occur. It was more likely that the observed second phase was a transient phase (corresponding to an incomplete segregation of the copper atoms during the rapid cooling process) quite different in composition from the equilibrium Zr_2Cu phase. This contention was consistent with the absence of distinct, identifiable Zr_2Cu reflections in the diffraction patterns obtained from the quenched alloys.

3.2. Mechanical properties of the beta-quenched alloys

It was found that even small additions of copper enhanced the strength of zirconium martensites considerably. Fig. 8 shows that the hardness of the dilute zirconium–copper martensites examined increased almost linearly with copper content. The strengthening brought about by copper additions was also reflected in the true stress versus true plastic strain plots obtained from room temperature tensile testing data (Fig. 9). The 0.2% offset yield strength and the ultimate tensile strength of these martensites showed a near-linear dependence on the square roots of the copper concentration in the corresponding alloys (Fig. 10). The temperature dependence of the yield stress and of the flow stress at 5% true plastic strain is illustrated in Fig. 11 for the two most dilute alloys. Typical dislocation structures, obtained in the deformed martensites, are illustrated in Fig. 12.

The enhanced strength of the dilute zirconium–copper martensites (in comparison with the martensite in unalloyed zirconium) could be due partly to solid solution effects and partly to substructural changes brought about by copper addition. Since there is a large disparity in the atomic sizes of zirconium and copper, a copper atom in the zirconium lattice would give rise to severe localized lattice distortions. In view of this, a significant hardening effect would be expected when zirconium is supersaturated with copper. That copper can be regarded as an effective solid-solution strengthener in zirconium also follows from the physical principles of solid-solution hardening discussed by Stern [11] in the context of

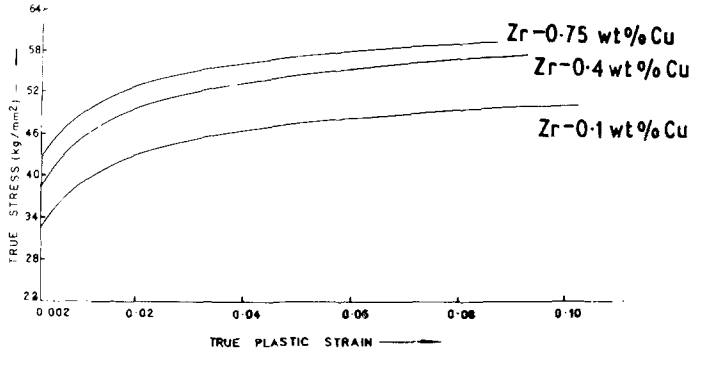

Figure 9 True stress versus true plastic strain plots (at room temperature) for three dilute zirconium–copper martensites.

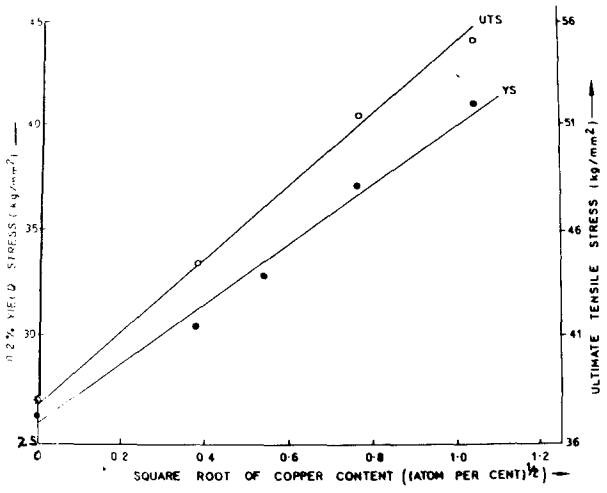

Figure 10 Near linear dependence of the 0.2% offset yield strength and the ultimate tensile strength on the square root of copper content in dilute zirconium–copper martensites.

titanium alloys. In zirconium alloys, as in the case of titanium alloys, it can be expected that solution hardening is a local electronic effect where important interactions occur within an interatomic distance of the solute atom. Since copper ([Ar] $3d^{10}4s^1$) is quite a few columns apart from zirconium ([Kr] $4d^2 5s^2$) in the periodic table, the perturbation of the wave function of zirconium due to the presence of copper would be appreciable. In the present work, the observation of lath boundary precipitates in the quenched alloys indicated that the catharsis of copper atoms from the zirconium lattice could not be suppressed during the beta-quenching treatment and that the extent of supersaturation in the martensite produced was smaller than that implied by the corresponding alloy composition. However, the equilibrium solubility of copper in alpha-zirconium being negligible at room temperature, the gradual decrease in the volume of the unit cell of the α-Zr(Cu) solid solution with increasing copper additions implied that the martensites were supersaturated to some extent and that the degree of super saturation increased with increasing solute concentration in the alloys. In view of these considerations, it was felt that solid-solution hardening was one of the major factors contributing to the strength of these martensites. However, no quantitative assessment of this contribution could be made. The observed near-linear variation of the yield stress with the square root of the copper concentration in the alloys suggested that the mechanism of solid-solution hardening could be similar to that implied in the model proposed by Fleischer [12]. This model assumes a localized interaction between the solute atoms and the lattice, giving rise to a tetragonal distortion resulting in a rapid hardening of the lattice and predicts that the rate of solution

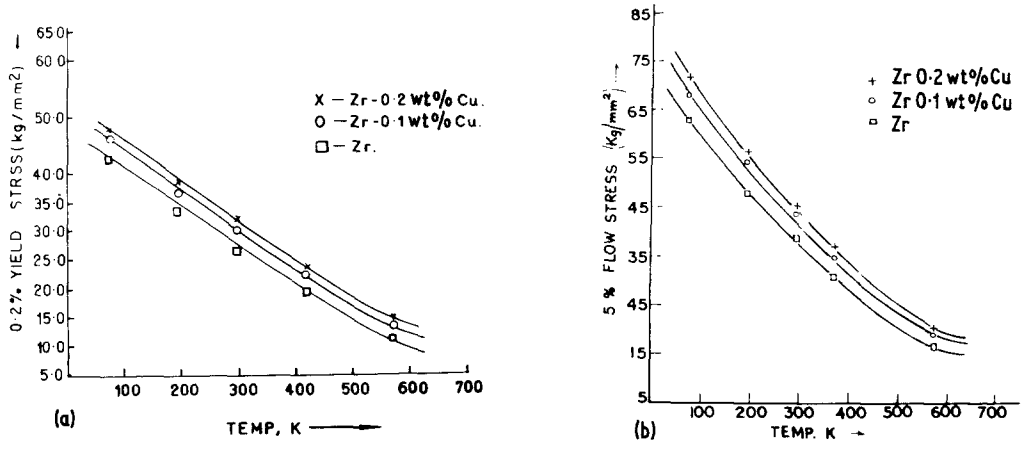

Figure 11 The temperature dependence of (a) the yield stress and (b) the flow stress at 5% true plastic strain in two dilute zirconium–copper martensites.

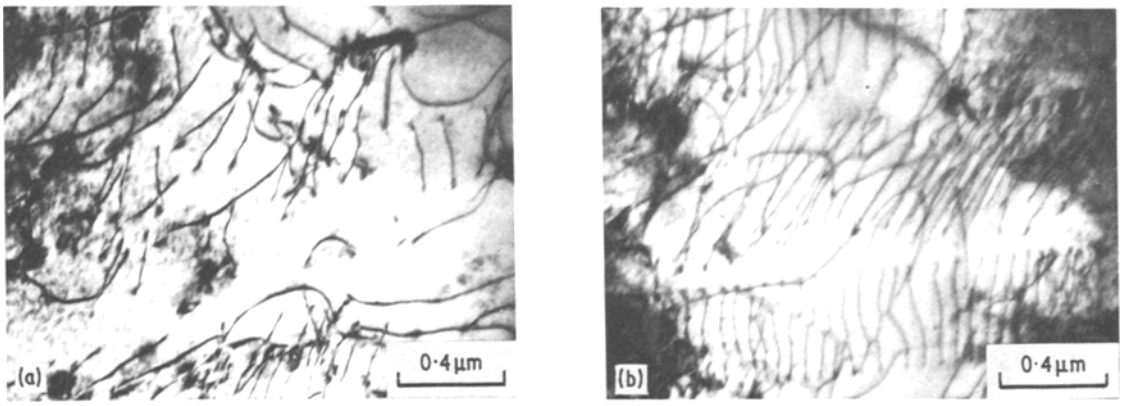

Figure 12 Typical dislocation structures obtained on deforming the beta-quenched alloys; (a) Zr–0.1 wt % Cu.

hardening should be temperature-dependent. In the present work no attempt was made to examine the temperature dependence of the solid-solution hardening of the martensites. The situation here was complicated by the partial solute rejection from the solvent lattice. The extent of this rejection could not be assessed quantitatively and, therefore, it was not possible to determine the amount of copper that actually remained in solution in the different alloys. In view of these difficulties, it was not possible to establish the operating solution-hardening mechanism.

It was observed that the morphology and the substructure of the dilute zirconium–copper martensites were not much different from those of the unalloyed zirconium martensite, except for the presence of precipitates at the lath boundaries of the former. Within the range of compositions studied, there was no drastic change either in the lath size or in the density and the distribution of the intra-lath dislocations with increasing copper additions. In the context of zirconium–titanium martensites, it has been shown [13, 14] that lath boundaries do not contribute significantly to the strength of the martensite since they are not effective barriers to the propagation of dislocations and of deformation twins. In the present case, it was felt that the enhanced strength of the zirconium–copper lath martensites was partly due to the fact that the lath boundary precipitates rendered the boundaries relatively impenetrable against the motion of deformation fronts. It appeared that as the precipitate density and the average precipitate size (and thus the volume fraction of the precipitate phase) increased with increasing copper content of the alloys, the degree of impenetrability associated with the boundaries also increased. The situation could also be looked at from the point of view of the Hall–Petch relation

$$\sigma_f = \sigma_i + kd^{-1/2} \quad (1)$$

which expresses the flow stress in terms of the friction stress σ_i, the grain size d, and a constant k. It has been found that for small angle boundaries (such as lath boundaries) the value of the constant k is small (typically of the order of $\sim 0.2\ \mathrm{kg\,mm^{-3/2}}$ compared with $\sim 1\ \mathrm{kg\,mm^{-3/2}}$ for high angle grain boundaries [15]). The lath boundary precipitates in the present case appeared to cause the value of k to increase and thus strengthen the martensite. With increasing copper content, though the lath size did not decrease substantially, progressive hardening occurred since the increasing volume fraction of the precipitate phase led to a progressive rise in the value of k.

The observed variation in the values of the yield stress and the flow stress at 5% true plastic strain with changes in test temperature (Fig. 11) indicated that thermal activation was an important factor in relation to the deformation behaviour of these martensites. The nature of the curves also suggested that the addition of copper affected mainly the athermal component of the flow stress. This observation was consistent with the generally accepted view that substitutional solute atoms in titanium and zirconium mainly affect the athermal component of the flow stress [16, 17].

An attempt was made to analyse the work-hardening behaviour of these dilute zirconium–copper martensites in terms of the concepts developed by Ashby [18], in relation to the behaviour

of plastically inhomogeneous materials. It was felt that since the mean spacing between the partitioning interfaces (lath boundaries decorated with precipitates) was small in these martensites, the geometric slip distrance was also small so that the density of the geometrically necessary dislocations was far in excess of the "statistically stored" dislocations. Fig. 13 shows the plots of the flow stress, σ, against the square root of the true plastic strain, $\epsilon_p^{1/2}$, for three alloy compositions. In the case of each alloy, the plot consisted of two linear segments, with a transition in slope at about 2.5% true plastic strain. The rapid work-hardening at low strains (<2.5%) could be attributed to a sharp rise in the long-range internal stress during initial straining. However, not much significance need be attached to this high work-hardening rate because the initial portion of the flow curve could correspond to the localized flow of some regions of high stress concentration. The parabolic stress–strain behaviour at higher strains (>2.5%) suggested that at these strains the flow behaviour of the martensite was controlled by geometrically necessary dislocations and that the work-hardening in this regime could be expected to have been governed mainly by the short-range interaction of the gliding dislocations with the geometrically necessary ones. Ashby's one parameter work-hardening expression [18] for a polycrystalline material, partitioned by interfaces could be expressed as

$$\sigma = \sigma_0 + C\mu(b/\lambda)^{1/2}M^{3/2}\epsilon_p^{1/2} \qquad (2)$$

where σ and σ_0 are respectively the flow stresses at strains ϵ_p and zero, μ is the shear modulus, M is an appropriate orientation factor, b is the Burger's vector, λ is the geometric slip distance (which is determined by microstructure and is independent of strain) and C is a dimensionless constant. Equation 2 shows that the slope of the σ versus $\epsilon_p^{1/2}$ line has an inverse dependence on $\lambda^{1/2}$ and is determined, at any given strain, by the work-hardening rate

$$\frac{d\sigma}{d\epsilon_p} = \tfrac{1}{2}C\mu(b/\lambda)^{1/2}M^{3/2}\epsilon_p^{-1/2}. \qquad (3)$$

It was observed (Fig. 13) that this slope was almost the same for the martensites of the three compositions considered (at strains exceeding about 2.5%). This suggested that the precipitate-decorated lath boundaries controlled the accumulation of geometrically necessary dislocations and thus determined the work-hardening behaviour. Since the lath size did not change appreciably with changes in copper concentration in these alloys, the near equality of the slopes would necessarily follow in such an event. The lath boundary precipitate phase, a precursor to the Zr_2Cu phase, could be considered to be non-deformable in comparison with the softer α-Zr (Cu) solid solution and thus the boundaries would correspond to a distribution of non-deformable regions in a soft matrix; a situation where Ashby's theory is applicable.

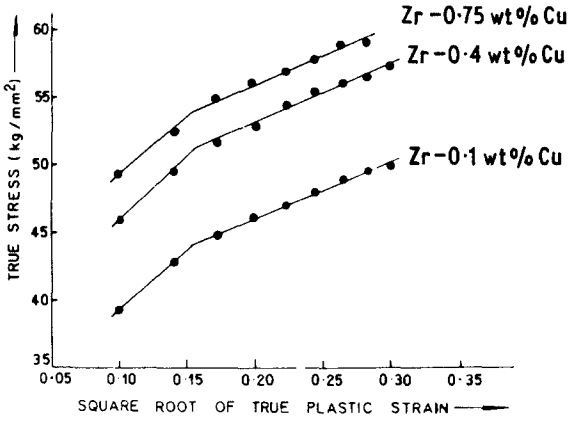

Figure 13 Plots of the true stress versus the square root of the true plastic strain for three dilute zirconium–copper martensites.

4. Conclusions

The following conclusions were reached:

(a) The martensite produced by rapidly quenching dilute zirconium–copper alloys from the beta-phase had a lath morphology and a dislocated substructure. Precipitation at the lath boundaries could not be suppressed by this quenching treatment. These precipitates, however, did not have the stoichiometry of equilibrium Zr_2Cu.

(b) Even small additions of copper enhanced the strength of zirconium martensites considerably. This strengthening was due both to solid-solution hardening and to the distribution of precipitates at the lath boundaries.

(c) The work-hardening behaviour of dilute zirconium–copper martensites could be analysed in terms of Ashby's theory of the deformation of plastically inhomogeneous materials.

(d) The temperature dependence of the flow stress at any given level of plastic strain indicated that the addition of copper enhanced mainly the athermal component of the flow stress.

Acknowledgements

The authors are grateful to Mr C. V. Sundaram and Dr M. K. Asundi for their keen interest in this work and to Dr R. Krishnan and Dr S. Banerjee for many useful discussions.

References

1. M. ARMAND, H. DEMARS and J. P. GIVARD, *Rev. Met.* 64 (1967) 249.
2. J. M. FRENKEL and M. WEISZ, International Conference on Use of Zirconium Alloys in Nuclear Reactors (Marianske Lazne, 1968).
3. P. BARQUE and R. DARRAS, Canadian Patent No. 750318 (1967).
4. Associated Electrical Industries, French Patent No. 1 281 191, (1961).
5. M. HANSEN and K. ANDERKO, "Constitution of Binary Alloys", (McGraw–Hill, New York, 1958).
6. E. TEATUM, K. GSHNEIDER Jr and J. WABER, Los Alamos Scientific Laboratory Report No. LA-2345 (1960).
7. M. L. PICKLESIMER, ORNL-3160 (1961).
8. S. BANERJEE and R. KRISHNAN, *Met. Trans.* 4 (1973) 1811.
9. J. C. WILLIAMS, R. TAGGART and D. H. POLONIS, *Met. Trans.* 1 (1970) 2265.
10. J. C. WILLIAMS, D. H. POLONIS and R. TAGGART, "The Science, Technology and Application of Titanium", edited by R. I. Jaffee and N. E. Promisel (Pergamon Press, Oxford, 1970) p. 733.
11. E. A. STERN, in "Physics of Solid Solution Strengthening", edited by E. W. Collings and H. L. Gegel (Plenum Press, New York, 1973) p. 183.
12. R. L. FLEISCHER, *J. Appl. Phys.* 33 (1962) 350.
13. S. BANERJEE, S. J. VIJAYAKAR and R. KRISHNAN, *Acta Met.* 3, to be published.
14. S. BANERJEE, Ph.D Thesis, Indian Institute of Technology, Kharagpur (1973).
15. R. B. NICHOLSON, in "Strengthening Methods in Crystals" edited by A. Kelly and R. B. Nicholson (Elsevier, Amsterdam, 1971) p. 535.
16. K. R. EVANS, *Trans. TMS-AIME* 242 (1968) 648.
17. G. A. SARGENT and H. CONRAD, *Scripta Met.* 4 (1970) 129.
18. M. F. ASHBY, in "Strengthening Methods in Crystals", edited by A. Kelly and R. B. Nicholson (Elseiver, Amsterdam, 1971) p. 137.

Received 28 April and accepted 8 June 1978.